Journal of Visualization, Vol. 11, No. 1 (2008)71-78

Regular Paper

Imaging and Diagnostics of Turbulent Methane-Air Premixed Flames by Acetone-OH Simultaneous PLIF

Nakamura, Y.*[1], Manome, S.*[2] and Yamashita, H.*[3]

*1 Division of Mechanical and Space Engineering, Hokkaido University, N 13 W 8, Kita-ku, Sapporo 060-8628, Japan. E-mail: yuji-mg@eng.hokudai.ac.jp
*2 Toho Gas Co. Ltd, 19-18, Sakurada-cho, Atsuta-ku, Nagoya 456-8511, Japan.
*3 Department of Mechanical Science Engineering, Nagoya University, Furo-cho, Chikusa-ku, Nagoya 464-8603, Japan.

Received 28 August 2007
Revised 15 November 2007

Abstract : A strategy of diagnostics of ultra-lean combustion based on acetone-OH simultaneous PLIF is presented. Acetone seeded in the fuel flow and combustion-generated OH work for a marker of "unburned" and "burnt" zones, respectively. Since acetone and OH does not coexist when the proper combustion takes place, the signal "valley" (dark zone) between acetone and OH fluorescence can be detected, which corresponds to flame zone; representative of the combustion status. System required for current imaging technique is *one*-laser and *one*-detector combination with "turned" band-pass filter. Transmittance characteristics of the filter and acetone-seeding rate are key issues to attain clear imaging, and we found that there is proper combination of them for that purpose. Imaging demonstration for the turbulent premixed flames shows the usefulness and applicability of this scheme on complex flame diagnostics: unique flame broken flame structure ("unburned" or "burnt" islands exist separately) are clearly obtained by this approach.

Keywords : Flame imaging, PLIF, Acetone, OH, Turbulent flame.

1. Introduction

It is important to develop the low-emission combustor to reduce harmful products (such as nitric oxide, particulate matter etc.) as well as increase the energy conversion efficiency. Ultra-lean combustion is one of the distinctive candidates to attain such requirements (Hayashi et al., 2000). However, ultra-lean combustion essentially works near the extinction limit, we have to manage the combustion instability. Although the excellent laser diagnostics to access multi-dimensional radical structure as well as the status in the flame has been extensively developed (e.g., planar laser-induced fluorescence: PLIF), diagnostics of extremely lean condition is still a challenging matter. For example, to predict the heat release performance in the flame, CH-PLIF has been often applied because CH is known to exist only in thin heat release zone (Allen et al., 1986, Chen et al., 1997). It is pointed, however, that CH-PLIF may fail under very lean condition (equivalence ratio, ϕ, is less than 0.65, for methane-air premixed flame), at which CH is severely produced (Tanahashi et al., 2003). As alternative, CH_2O-OH PLIF has been developed (Paul and Najm, 1998; Bockle et al., 2000; Vagelopoulos and Frank, 2005) on the basis that the heat release zone corresponds to multiples of their concentration: $[CH_2O][OH]$, however, it always requires multiple lasers and detectors to increase the system cost and complexity.

To overcome above demerit, acetone-OH simultaneous PLIF has been developed by authors recently (Nakamura et al., 2005a and 2005b; Manome et al., 2007). This scheme is to look for "unburned" and "burnt" zones simultaneously via fuel-seeded acetone and combustion-generated OH, respectively, then "indirectly-visualize" the flame zone sandwiched by them (see Fig. 1). Considerable amount of acetone and OH exist in combustion field until the extinction, this scheme could be applied for diagnostics of ultra-lean combustion. Original idea of acetone-OH simultaneous PLIF was proposed by Hanson's group (Seitzman et al., 1994) by using multiple lasers and detectors, to visualize mixing zone in high-speed turbulent flow. Later, they developed one laser and two detectors combination to apply to the diagnostics of turbulent diffusion flames (Yip et al., 1994). Tamura et al. (1998 and 2000) first applied this scheme to premixed flames with two-lasers and two-detectors combination, but their interest was to obtain combustion area and no attempt was made to look for the local flame structure. In 2005, we first applied to look for the local flame structure in laminar premixed flame and successfully made the clear imaging of the thickness of flamelet with local curvature (Nakamura et al., 2005a and 2005b) via "one-laser and one-detector combination" system. So far, it has been understood that the visualized "flame zone" given by this scheme as non-fluorescence zone can well correlates to so-call preheated zone and the thickness is well matched to the burning rate according to 1-D theoretical data. Capability of present technique to the turbulent flame diagnostics has been briefly pointed (Manome et al., 2007). To get clear imaging, selection of tracer and band-pass filter mounted in front of detector is vital, however, no detail description for such technical issue has not been provided yet. In this paper, the effect of transmittance character of the applied filter on imaging is investigated to understand the best choice to apply for the diagnostics of ultra-lean combustion. Additionally imaging demonstration of forced turbulent flames is performed to show the capability of this scheme on complex flame diagnostics.

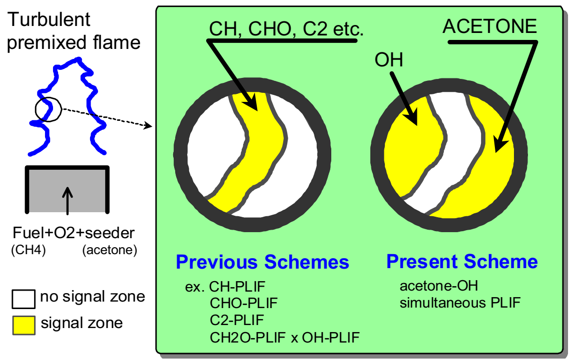

Fig. 1. Schematic illustration of way to visualize flame zone.

2. Experiment

2.1 How to Work and What is Needed?

As is well-known, acetone has broad absorption band in the range of 225-320 nm (precisely it depends on the field temperature (Thurber et al., 1998)). An important fact is that most OH absorption line (~283 nm) is within the range. Technically speaking, therefore, single line (~283 nm) can excite both acetone and OH simultaneously. Now we must aware the difference of quantum yield of OH and acetone; possibly fluorescence intensities are different. This could bring some difficulties to visualize both fluorescence signals at similar level by single detector. There are two ways to control this: one is to select appropriate band-pass filter (which allows to transmit both fluorescence from acetone, about 300-500 nm, and OH, around 308 nm) and the other is to adjust the seeding amount of acetone. This concern suggests that most "effective" combination of the seeding rate of acetone (i.e., tracer gas) and band pass filter may exist. By the way, acetone is not only candidate of tracer gas and any kind of fuel flow (we consider methane-air flame here, as described in later) is applicable for this visualization technique inherently.

2.2 Experimental Apparatus

Since details of the experimental apparatus are found in elsewhere (Nakamura et al., 2005a and 2005b), only a brief description is made here. Figure 2 shows experimental apparatus used in this study. Laser system consists of the combination of Nd:YAG (GCR-230, Spectra Physics Inc.) and Dye laser (HD-300, Lumonics Inc.). Frequency doubled Nd:YAG laser (532 nm, 10 Hz, 5 ns of pulse) is turned to 566.4 nm by Dye laser, then converted to 283.2 nm with BBO crystal. This selected line (283.2 nm) corresponds to OH absorption line of $A^2\Sigma^+ <- X^2\Pi$ transition ((1,0) band of $Q_1(7)$). As mentioned previously, this is within the absorption band spectra of acetone (225 nm-320 nm). The wavelength-tuned laser beam is transformed to the thin sheet by lens system as shown in the figure. Laser power directly introduced into the flames is approximately 5-10 mJ.

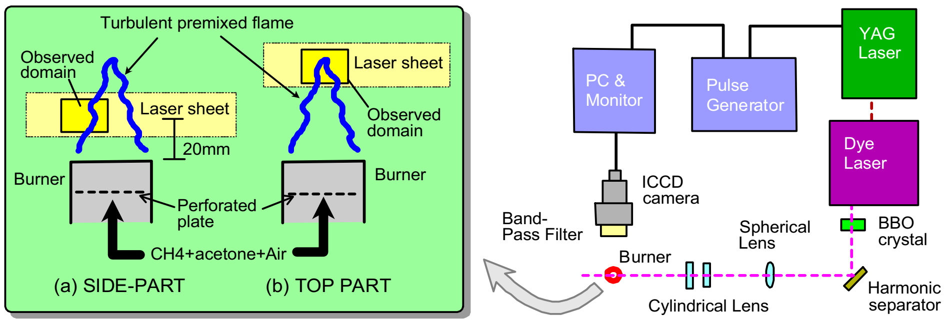

Fig. 2. Experimental apparatus (right) and visualized domain (left).

Fluorescence signals are detected by intensified-CCD (C4272&C4274, Hamamatsu Photonics Corp.) with the band-pass filter. Imaging range is 36.5 mm x 29.0 mm and corresponding pixel number is 640 x 480, respectively, and minimum spatial resolution is 0.06 mm/pixel. Image center is fixed as indicated in Fig. 2. Pulse generator (DG535, SRS Inc.) is used for timing control of the entire system.

Laminar and turbulent methane-air premixed flames established over Bunsen-type of burner (inner diameter is 27 mm) are used as the reference flames. The turbulence is generated by the perforate plate (Yamamoto et al., 2003). Acetone is seeded by bubbling method and seeding stability is well-checked in the preliminary test. Small pilot flames are set around the burner exit to avoid blow-off. Fuel supply rate of the pilot flames is much smaller than that of the main flow (~0.1 % in volume), thus it does not play a role on the main flame behavior.

2.3 Experimental Conditions

Total flow rate is fixed at 1000 cm^3/s throughout the study. Average flow velocity is 175 cm/s. Imposed turbulence intensity, u_t, is 13.5 cm/s and turbulence (integral) scale is 3.5 mm generated by the perforated plate, suggesting the present turbulent flames are categorized in laminar flamelet regime. Considered equivalence ratio of the mixture is varied from $\phi = 0.77$ to $\phi = 1.27$. Note that acetone is combustible gas species and can act as fuel, therefore, the equivalence ratio shown here is calculated for the methane-acetone-air mixture. Base condition applied is $\phi = 0.86$; corresponding volumetric flow rate of acetone and methane are 10.25 cm^3/s and 63.26 cm^3/s, respectively. In the followings, if no special description is made, this base condition is applied. Uncertainty of the experimental results is less than 10 % according to our previous study (Manome et al., 2007).

In this study, three series of experiments are performed. First, effect of exposure time duration of the detector (from 200 ns to 100000 ns) on imaging is investigated to ensure how to eliminate of the chemiluminescence signal (i.e., background noise) from the flame. Second, effects of acetone seeding amount and band-pass filter on imaging are discussed. Lastly, instantaneous 2-D imaging of flame zone in lean turbulent flames is demonstrated and observed unique features are discussed.

3. Results and Discussion

3.1 Effect of Exposure Time Duration on Imaging (Elimination of Chemi-Luminescence Signal)

Figure 3 compares the effect of gain level on the maximum signal intensity of chemiluminescence in various exposed time durations (Δt = 200 ns, 500 ns, 30000 ns) in flames of $\phi = 0.86$ mixture. Applied band-pass filter is C (details are described in later), which is the same one used in our previous studies (Nakamura et al., 2005a and 2005b). Fluorescence signal with Δt = 200 ns is also added in the figure. As indicated, every signal has certain level of background noise about 30 a.u. As expected, every signal intensity increases in higher gain level. As the time duration becomes shorter, the difference in intensity between fluorescence and chemiluminescence becomes larger, suggesting that clear imaging (high signal-to-noise ratio; S/N) could be attained. Since the chemiluminescence signals in Δt = 200 ns and 500 ns almost remain as constant against the applied gain level, the difference from the fluorescence signal is apparent when the higher gain is applied. On the contrary, for the case of the larger time duration (Δt = 30000 ns), signal intensities of chemiluminescence and fluorescence give similar curve irrespective of the applied gain level, implying that elimination of chemiluminescence would be failed. Overall, once initial background noise (30 a.u. in this system) is properly removed, imposing larger gain level (> 2.5) with shorter exposed time duration (less than Δt = 500 ns) would be preferred in the present system to get clear imaging of reactive zone in premixed flames (interested signal intensity is at least 10 times larger than the residual noise).

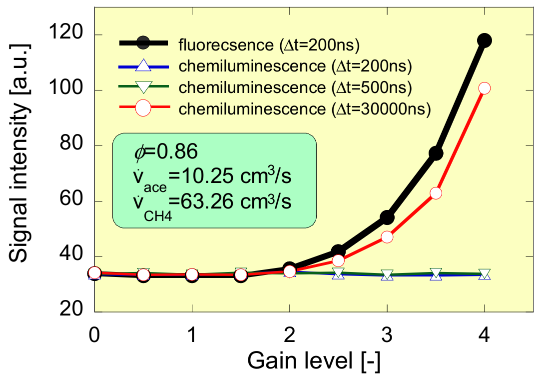

Fig. 3. Effect of gain on signal intensities.

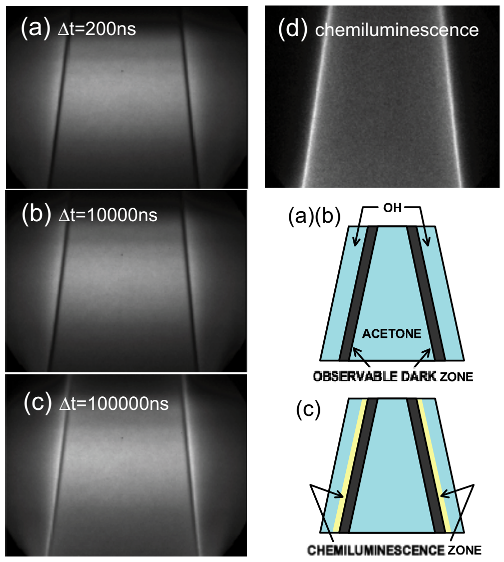

Fig. 4. Effect of exposure time durations on imaging.

2-D PLIF images in various exposure time durations (Δt = (a) 200 ns, (b) 10000 ns, (c) 100000 ns) are shown in Fig. 4. Imposed condition is ϕ = 0.86 without perforated plate (i.e., laminar premixed flame). Image center is on burner axis and 20 mm above the burner surface. 2-D chemiluminescence image (without laser input, milli-second exposure time) are also shown for the comparison purpose in (d). From the figure, (a) and (b) shows almost no difference; this is quite reasonable since the excitation laser pulse duration is nearly 5 ns and subsequent fluorescence lifetime is a couple tens nano-seconds (< 200 ns). Considering altogether, as long as the chemiluminescence signal is properly eliminated, fluorescence image may not vary with the exposure time duration in the order of hundreds nano-seconds. On the contrary, in extremely longer exposure time duration (c), chemiluminescence is no longer eliminated and observed image consists of mixed signals of fluorescence and chemiluminescence.

One important fact is also confirmed that observed dark zone thickness becomes narrower and brightness is increased near the outer edge of the dark zone in (c). This could be because that chemiluminescence is overlapped outer region of the dark zone (see inserted illustration in Fig. 4). According to the previous numerical predictions (Yamamoto et al., 2003), it has been known that the location of CH peak (~ chemiluminescence peak) corresponds to nearly half of OH maximum, where outer edge of the dark zone.

3.2 Effect of Band-Pass Filter and Tracer Amount on Imaging of Flame Zone

As mentioned in earlier, for simultaneous imaging of acetone and OH in single detector, their magnitude of signal intensities must be equal or similar level at least. Such requirement can be expressed by the following formula:

$$\int \tau(\lambda)\cdot I_{ace.}(V_{ace.},\lambda)d\lambda \approx \int \tau(\lambda)\cdot I_{OH}(\phi,\lambda)d\lambda \quad (1)$$

where τ, λ, I_i and $V_{ace.}$ denote the spectral transmittance of the band-pass filter set to the detector, wavelength, spectral fluorescence intensity of i_{th} species (i = OH and acetone in the present study) and volumetric flow rate of seeded acetone, respectively. Spectral fluorescence intensity of acetone ($I_{ace.}$) is a function of acetone seeding amount (~ $V_{ace.}$) and wavelength (λ) (Lozano et al., 1992; Bryant et al., 2000). I_{ace} is also affected by field temperature, however, such effect is neglected here, since the dependency is comparably small. Spectral fluorescence intensity of OH (I_{OH}) is a function of imposed equivalence ratio (ϕ) and wavelength (λ). Since excitation line is 283.2 nm which corresponds to Q-branch in OH, temperature dependency is minimized. Parameters included above formula are now summarized as following three quantities: τ, $V_{ace.}$, ϕ. If we change equivalence ratio of the mixture by modifying the acetone-seeding amount, ϕ can be expressed by ϕ ($V_{ace.}$), then parameters can be reduced to two (τ, $V_{ace.}$). This means that these two quantities are not freely determined, suggesting that there is proper combination of the imposed filter characteristics and seeding amount of the tracer (acetone). To check the filter effect on imaging, we consider four different filters (A, B, C and D) with various acetone-seeding conditions (hence, various equivalence ratios). Figure 5 shows transmittance curves of the tested filters. For comparison purpose, fluorescence spectra from acetone and OH (Nakamura et al., 2005b) are also shown in (a). Note that these four filters have difference transmittance characters in OH fluorescence regime; transmittance becomes larger in alphabetical order (A to D).

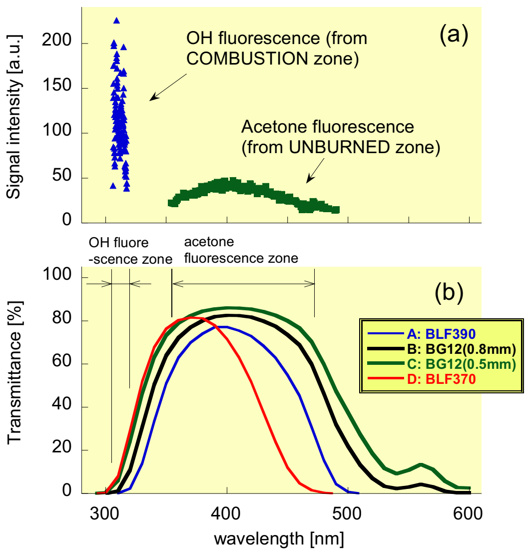

Fig. 5. (a) Fluorescence spectra of OH and acetone and (b) transmittance spectra of tested filters (A-D), ϕ = 0.86.

Figure 6 shows the effect of band-pass filter and seeding amount of acetone on 2-D PLIF image of laminar premixed flames in various mixture conditions (ϕ = 0.77, 0.97, 1.27). Applied gain level is indicated in the figure for the reference purpose. It is known that filter A does not show any OH fluorescence signal and no use for the present visualization scheme. By filter D, acetone signal becomes rather weak and larger amount of acetone seeding is required to work. By filter B, acetone signal is transmitted too much when large amount of acetone is introduced in the fuel flow, suggesting that this would be suitable for little amount of acetone seeding condition. Filter C could work for wide range of acetone seeding amount.

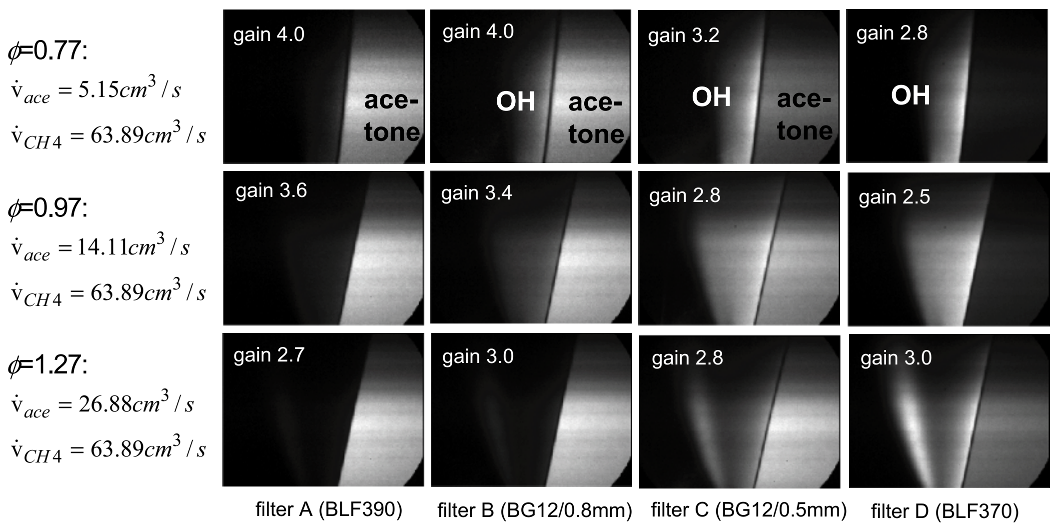

Fig. 6. Obtained 2-D acetone-OH fluorescence images given by different filters.

As mentioned previously, acetone is combustible component and acts as fuel. Although we have confirmed that burning velocity of the mixture does not change much in the wide range of acetone-seeding amount as seen in Fig. 7, precise flame character might be different from the original mixture (= without acetone-seeding) through the difference in specific heat and transport properties of the mixture, for example. In this sense, it is preferable to reduce the seeding amount as much as possible (Degardin et al., 2005). In such case, filter B would be the best choice for $\phi = 0.77$ although the high S/N would be sacrificed (applied gain level must be larger, though). When we consider the ultra-lean condition at which produced OH might be further decreased, then filter C with high gain is expected to work properly. Once we have other candidate for the tracer gas beyond acetone (e.g., fluorescence intensity of naphthalene is higher than acetone for 266 nm of excitation (Hirasawa et al., 2007)), the seeding amount can go further smaller. If the targeted mixture condition is fixed, we should fixed the seeding rate of tracer and apply the special designated filter whose the transmittance performance is artificially controlled. Transmittance character of B and C can be the reference for this purpose.

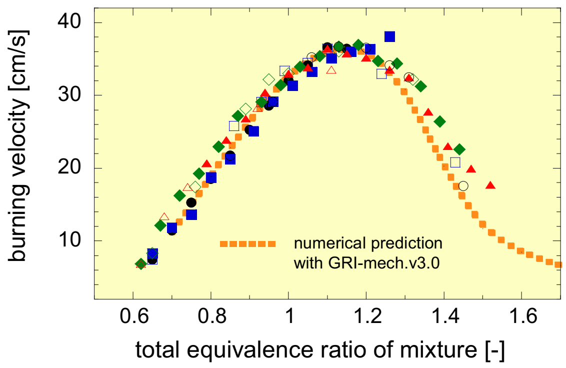

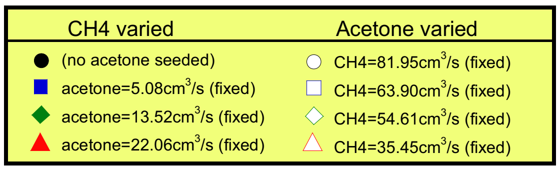

Fig. 7. Measured burning speed of various mixture of methane-acetone-air premixed flames (numerical prediction by GRI-mech 3.0 is added for comparison purpose).

3.3 2-D Imaging of Flame Zone in Lean Turbulent Premixed Flames

Figure 8 shows instantaneous 2-D PLIF images of lean turbulent flames ($\phi = 0.84$ with volumetric flow rate of acetone and methane is 5.08 cm³/s and 71.84 cm³/s, respectively) with filter C. This condition is selected because it could ensure both clear imaging (due to higher equivalence ratio) and less effect of acetone-seeding on combustion status, e.g., burning velocity (see Fig. 7: data of 5.08 cm³/s of acetone-seeding flow rate (closed square) is relatively close to closed no acetone-seeding case (closed circle)).

In the figure, (a)-(d) show the magnified images at the side part of the flame (see Fig. 2(a)), whereas (e)-(h) show the magnified images at the top part of the flame (see Fig. 2(b)). Cusp formation is clearly observed in (a) and (e), which is one important characters of turbulent flame in laminar flamelet regime (Williams, 1985). Strange unburned "arm" structure is found in (b) which can be frequently observed in turbulent flames (e.g., Tanahashi et al., 2005). A "unburned island" structure as shown in (c), (d), (f) and a "burnt island" as shown in (d) are clearly captured, which is expected by previous theoretical works (ex. Chen et al., 1999; Nada et al., 2004). Detection of such "island" structure is important to understand complex turbulent combustion nature. For example, there must be local extinction process during the formation of "unburned island" (Renard et al., 1998). This fact suggests that this scheme could be applicable for diagnostics of near-extinction behavior in ultra-lean combustion. By the way, determination of "unburned" or "burnt" zone is easily made when the imposed turbulent condition is relatively weak (see the corresponding movie available at http://york-me.eng.hokudai.ac.jp/~yuji/AcetoneOH_PLIF_movie). For strong turbulent condition, however, the same treatment may fail and special care must be taken. One candidate is to use colored CCD camera with Image Intensifier: it could image each fluorescence zone with different color output. Additional optical system (such as "stereo viewer (Nakayama et al., 1999)") may also work for this purpose. Further system tuning would be made in our future study.

Additionally, "dark spot" is often found in the unburned area as shown in (g) and "OH spot" without any surrounding dark zone are found in (h). They might be the result of either stronger distortion by the turbulent flow or complex 3-D flame configuration appeared in the observable plane (e.g., projecting flame goes across to the imaged plane normally, e.g., Nada et al., 2004). Once the "unburned island" is formed like (c), separated unburned gas surrounded by burnt gas is consumed as combustion progresses and finally the area becomes “OH spot”. We have captured such instance in (g): bright OH spot indicates inhomogeneous burned spot and its brightness might be related to the lifetime of OH. In the same manner, the “burned island” appeared in the unburned zone would finally become “dark spot” as seen in (g); the local temperature at dark spot would be high enough to decompose acetone but low enough to generate OH. Although other possibility could be counted, it is worthy to note that this scheme is applicable to access such complex combustion behavior.

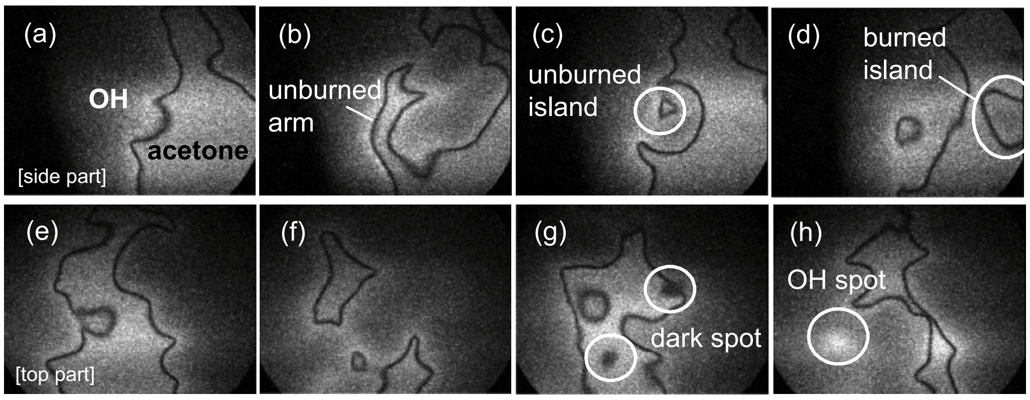

Fig. 8. 2-D acetone-OH PLIF images for turbulent premixed flame ($\phi = 0.84$), (a)-(d) side portion, (e)-(h) top portion (see Fig. 2).

4. Conclusion

Imaging of flame zone in laminar and turbulent premixed flames by applying acetone-OH simultaneous PLIF is demonstrated and applicability of the present scheme to the diagnostics of lean turbulent premixed combustion is pointed. Elimination of background noise by manipulating exposed time duration in detector is effective. Effects of band-pass filter which is a key part in this visualization scheme and seeding amount (rate) of tracer on clear imaging is precisely revealed and best combination is suggested by manipulating its transmittance performance. 2-D instantaneous PLIF images on turbulent premixed flame case reveal clear cusp formation, "unburned" and "burnt" island structures, separately dark and OH spots, showing that applicability of the this scheme on complex turbulent structure near the extinction condition.

Acknowledgments

This work is partially supported by Tanikawa-Netsugijyutu foundation and Yoshida foundation. YN express his sincere thanks to their supports to conduct this study.

References

Allen, M. G., Howe, R. D. and Hanson, R. K., Digital Imaging of Reaction Zones in Hydrocarbon-Air Flames using Planar Laser-Induced Fluorescence of CH and C_2, Optics Letter, 11-3 (1986), 126-128.

Bockle, S., Kazenwadel, J., Kunzelmann, T., Shin, D.-I., Schulz, C. and Wolfrum, J., Simultaneous Single-Shot Laser-Based Imaging of Formaldehyde, OH, and Temperature in Turbulent Flames, Proc. Combust. Inst., 28-1 (2000), 279-286.

Bryant, R. A., Donbar, J. M. and Driscoll, J. F., Acetone Laser Induced Fluorescence for Low Pressure/Low Temperature Flow Visualization, Exp. Fluids, 28-5 (2000), 471-476.

Chen, Y. C. and Mansour, M. S., Simultaneous Rayleigh Scattering and Laser-Induced CH Fluorescence for Reaction Zone Imaging in High-Speed Premixed Hydrocarbon Flames, Applied Physics B., 64-5 (1997), 599-605.

Chen, J. H., Echekki, T. and Kollmann, W., The Mechanics of Two-Dimensional Pocket Formation in Lean Premixed Methane-Air Flames with Implications to Turbulent Combustion. Combust. Flame, 116 (1999), 15-48.

Degardin, O., Renou, B. and Boukhalfa, A. M., Simultaneous Measurement of Temperature and Fuel Mole Fraction using Acetone Planar Laser-Induced Fluorescence and Rayleigh Scattering in Stratified Flames, Exp. Fluids, 40 (2006), 452-463.

Hayashi, S., Yamada, H. and Makida, M., Short-Flame/Quick -Quench: A Unique Ultralow Emissions Combustion Concept for Gas Turbine Combustors, Proc. Combust. Inst., 28-1 (2000), 1273-1280.

Hirasawa, T., Kaneba, T., Kamata, Y., Muraoka, K. and Nakamura, Y., Temperature Dependence of Intensities of Laser-Induced Fluorescences of Ethylbenzene and Naphthalene Seeded in Gas Flow at Atmospheric Pressure, J. Visualization, 10-2 (2007), 197-206.

Lozano, A., Yip, B. and Hanson, R. K., Acetone: a Tracer for Concentration Measurement in Gaseous Flows by Planar Laser-Induced Fluorescence, Exp. Fluids, 13 (1992), 369-376.

Manome, S., Nakamura, Y., Hayashi, N., Yamamoto, K. and Yamashita, H., Study of Acetone-OH Simultaneous PLIF for Combustion Diagnostics of Turbulent Flames, Trans. JSME Ser.. B., 73-725 (2007), 350-356.

Nada, Y., Tanahashi, M. and Miyauchi, T., Effect of Turbulence Characteristics on Local Flame Structure of H2–Air Premixed Flames, J. Turbulence, 5 (2004), 16.

Nakamura, Y., Manome, S., Yamashita, H. and Hayashi, N., Application of Simultaneous Acetone/OH PLIF Concept for Combustion Diagnostics, Proc. 6th World Conf. Exp. Heat Transfer, Fluid Mechanics, Thermodynamics (Sendai, Japan), (2005a-4), (CD-ROM) 6-b-2.

Nakamura, Y, Manome, S., Satomi, T., Hayashi, N. and Yamashita, H., Flame Diagnostics with Acetone-OH Simultaneous PLIF, J. Comb. Soc. Jpn., 47-142 (2005b), 290-299 (in Japanese).

Nakayama, H., Ishida, T., Kodama, Y. and Niimi, T., A study on a Method for 2-Dimensional Temperature Measurement Technique by O_2-LIPF (Development of a Stereo-Viewer and Verification of the Validity), JSME Int'l. J., 42-3 (1999), 547-552.

Paul, P. H. and Najm, H. N., Planar Laser-Induced Fluorescence Imaging of Flame Heat Release Rate, Proc. Combust. Inst., 27-1 (1998), 43-50.

Renard, P.-H., Rolon, J. C., Thevenin, D. and Candel, S., Wrinkling, Pocket Formation, and Double Premixed Flame Interaction Processes, Proc. Combust. Inst., 27-1 (1998), 659-666.

Seitzman, J. M., Miller, M. F., Island, T. C. and Hanson, R. K., Double-pulse Imaging using Simultaneous OH/Acetone PLIF for Studying the Evolution of High-Speed, Reaction Mixing Layer, Proc Combust. Inst., 25-2 (1994), 1743-1750.

Tamura, M., Sakurai, T. and Tai, H., Simultaneous Laser-Induced Fluorescence Imaging of Unburnt and Reacting Areas in Combustion Fields using a KrF Excimer Laser, Opt. Review, 5-2 (1998), 119-123.

Tamura, M., Sakurai, T. and Tai, H., Visualization of Crevice Flow in an Engine using Laser-Induced Fluorescence, Opt. Review, 7-2 (2000), 170-176.

Tanahashi, M., Tsukinari, S., Saito, T., Miyauchi, T., Choi, G.-M., Ikame, M., Kishi, T., Harumi, K. and Hiraoka, K., On the Sound Generation and its Control in Turbulent Combustion Field, Proc. 3rd Sympo. on Smart Control of Turbulence, (2002-3) (http://www.turbulence-control.gr.jp/sympo_j/FY2001/).

Tanahashi, M., Murakami, S., Choi, G.-M., Fukuchi, Y. and Miyauchi, T., Simultansous CH-OH PLIF and Stereoscopic PIV Measurements of Turbulent Premixed Flames, Proc. Combust. Inst., 30-1 (2005), 1665-1672.

Thurber, M. C., Grisch, F., Kirby, B. J., Votsmeier, M. and Hanson, R. K., Measurements and Modeling of Acetone Laser-Induced Fluorescence with Implications for Temperature-Imaging Diagnostics, Appl. Opt., 37 (1998), 4963-4978.

Vagelopoulos, C. M. and Frank, J. H., An Experimental and Numerical Study on the Adequacy of CH as a Flame Marker in Premixed Methane Flames, Proc. Combust. Inst., 30-1 (2005), 241-249.

Williams, F. A., Combustion Theory, 2nd ed., (1985), Addison-Wesley, Menlo Park, California.

Yamamoto, N., Nakamura, Y., Zhao, D. and Yamashita, H., Measurement of Flame Structure of Turbulent Premixed Flame by OH-PLIF, Fluid & Heat Eng. Res., 38 (2003), 19-28 (in Japanese).

Yip, B, Miller, M. F., Lozano, A. and Hanson, R. K., A Combined OH/Acetone Planar Laser-Induced Fluorescence Imaging Technique for Visualizing Combusting Flows, Exp. Fluids, 17 (1994), 330-336.

Author Profile

Yuji Nakamura: He received his M.Sc .(Eng) in Mechanical Engineering in 1995 from Nagoya University. He received his Ph.D. in 2000 from the same university. He worked at The University of Kentucky as visiting research assistant in 1996-1997. He joined in Department of Mechanical Engineering, Nagoya University as research associate (1998) and became assistant professor at Center for Integrated Research in Science and Engineering (2003) and EcoTopia Science Institute (2004), Nagoya University. He was invited at The National Institute of Standards and Technology (NIST) during 2000-2001 as visiting professor. He is currently associate professor at Division of Mechanical and Space Engineering, Hokkaido University since 2005. His research interests are Combustion, Fire Science, and Space Engineering.

Satoshi Manome: He received his M.Sc. (Eng.) degree in Mechanical Engineering in 2005 from Nagoya University and currently serves as sales engineer at Toho Gas Co. Ltd. During his master course in Nagoya University, he gave a talk on laser diagnostics in more than 10 conferences and prized Best Picture Award from The Combustion Society of Japan (2004.12) and Best Poster Award from ISETS05 (2005.8). He received Higashiyama-prize which is awarded to the most outstanding student in graduate course in Mechanical Engineering, Nagoya University out of 80

Hiroshi Yamashita: He received his M.Sc. (Eng.) degree in Mechanical Engineering in 1974 from Nagoya University and his Ph.D. in Mechanical Engineering in 1977 from the same university. He immediately joined in Department of Mechanical Engineering, Nagoya University as research associate (1977), then promoted to assistant professor (1979), associate professor (1983), and became professor (1998) at the same university. He joined at The National Institute of Standards and Technology (NIST) during 1990-1991 as visiting professor. He gave a number of invited talk on numerical combustion and has more than 150 journal papers in this field. His current research interests are Numerical Combustion, Combustion Modeling, and Catalytic Reaction.